

End-to-end Temporal Action Detection with Transformer

Xiaolong Liu^{1*} Qimeng Wang¹ Yao Hu² Xu Tang² Song Bai¹ Xiang Bai¹
¹Huazhong University of Science and Technology ²Alibaba Group
{liuxl, qimengwang, xbai}@hust.edu.cn, songbai.site@gmail.com
{yaoohu, buhui.tx}@alibaba-inc.com

Abstract

Temporal action detection (TAD) aims to determine the semantic label and the boundaries of every action instance in an untrimmed video. It is a fundamental task in video understanding and significant progress has been made in TAD. Previous methods involve multiple stages or networks and hand-designed rules or operations, which fall short in efficiency and flexibility. Here, we construct an end-to-end framework for TAD upon Transformer, termed TadTR, which simultaneously predicts all action instances as a set of labels and temporal locations in parallel. TadTR is able to adaptively extract temporal context information needed for making action predictions, by selectively attending to a number of snippets in a video. It greatly simplifies the pipeline of TAD and runs much faster than previous detectors. Our method achieves state-of-the-art performance on HACS Segments and THUMOS14 and competitive performance on ActivityNet-1.3. Our code will be made available at <https://github.com/xliu7/TadTR>.

1. Introduction

Video understanding has become more important than ever as the rapid growth of media prompts the generation, sharing, and consumption of everyday videos. As a fundamental task in video understanding, temporal action detection (TAD) aims to predict the semantic label, the start time, and the end time of every action instance in an untrimmed and possibly long video. For its wide range of applications, including security surveillance, home care, video editing, and so on, temporal action detection has gained increasing attention from the community in recent years [16, 21].

Most previous methods for TAD have complicated pipelines. As shown in Fig. 2, these pipelines involve multiple steps, such as segment scoring, proposal generation, action classification, and post-processing. While these methods achieve promising performance on standard

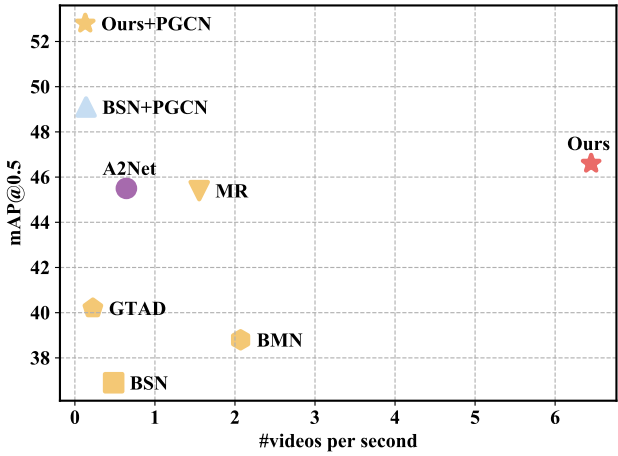


Figure 1. Comparison of recent temporal action detection methods on THUMOS14, in terms of both performance and speed. Our method achieves a good trade-off between efficiency and accuracy. When combined with a post-processing method PGCN [25], it achieves state-of-the-art performance.

benchmarks, there are several limitations. Firstly, the multiple steps may increase the time cost since they need to be carried out sequentially. Besides, some stages, such as the segment scoring stage, are time-consuming when there is a large number of candidates. Secondly, they can not enjoy end-to-end training, as some stages need to be trained independently or are not learnable (differentiable) (e.g. non-maximal suppression or grouping). As a consequence, multiple stages may accumulate errors and lead to sub-optimal results. Lastly, the hand-designed rules or operations also restrict flexibility.

In this paper, we propose a simple end-to-end temporal action detector. The detector adopts a set-prediction pipeline directly maps a set of learnable embeddings to action instances in parallel. To do that, we design a Transformer architecture that adaptively extracts the temporal context needed by each action prediction. The core is the temporal deformable attention layer that dynamically attends to a small number key locations in the video, which

*Work done during an internship at Alibaba Group.

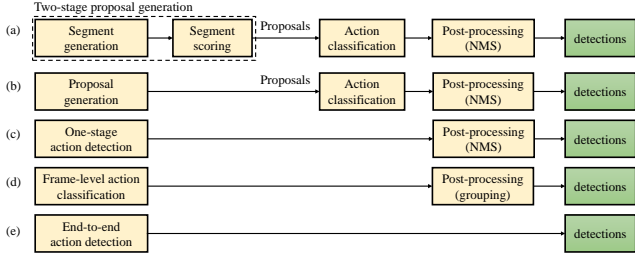


Figure 2. Comparison of different pipelines of temporal action detection. (a) Multi-stage pipeline in [16, 21] *etc.* (b) Two-stage pipeline in [20, 5]. (c) Top-down one-stage pipeline in [11], (d) Bottom-up one-stage pipeline in [24] (e) An end-to-end pipeline in this work.

saves the computation cost. It is more flexible than previous works that extracts context information by increasing the receptive field by a fixed ratio [6, 5]. It generates unique action predictions owing to a segment matching module that dynamically determines a one-to-one ground truth assignment during training, hence avoiding non-maximal suppression. The detector, dubbed as TadTR, achieves higher or competitive detection performance while running much faster than existing methods.

Specifically, TadTR achieves 46.6 mAP at IoU=0.5 on THUMOS14 [9], 31.32 average mAP on ActivityNet-1.3 [2] and 30.87 average mAP on HACS Segments [26]. Without bells and whistles, it achieves state-of-the-art performance on the recently introduced large-scale dataset HACS Segments. In terms of efficiency, it costs only 155 ms per video on average, which is significantly faster than recent state-of-the-art methods shown in Fig. 1. When combined with a post-processing method P-GCN [25], TadTR also achieves state-of-the-art performance on THUMOS14.

The contributions of this work are three-fold:

- We propose an set-prediction based detector that simplifies the pipeline for temporal action detection.
- We design a Transformer architecture that is able to adaptively capture temporal context for temporal action detection.
- Our method achieves the best or highly competitive results on standard datasets while running much faster than previous methods.

2. Related Works

Temporal Action Detection. Previous methods for temporal action detection can be roughly categorized into groups depending on the pipeline. (a) **Multi-stage methods** [21, 10]. They first generate candidate segments and train a binary classifier that associates each segment with a confidence score, resulting in proposals. Those proposals

with high scores are fed to a multi-class classifier to classify the actions. The candidate segments are generated by dense uniform sampling [16] or grouping local frames that may contain actions [12]. (b) **Two-stage methods** [20, 5] simplify the multi-stage pipeline by adopting a one-stage proposal generator, which directly predicts the scores and boundaries of pre-defined multi-scale anchors associated with each temporal location. These methods need to manually set multiple anchor scales, which restricts the flexibility. (c) **Top-down one-stage methods** [11] can be seen as the class-aware variant of the one-stage proposal generator. Recently, [22] augment the anchor-based one-stage detector with an anchor-free branch that makes predictions based on centers of actions. (d) A **bottom-up one-stage method** proposed in [24] first predicts the action and boundary probabilities and then groups frames with maximal structured sum as actions. We note that all the above methods require post-processing steps such as NMS or grouping, which prevent end-to-end learning.

An early work by [23] proposes an end-to-end temporal action detector based on recurrent neural networks (RNN) and reinforcement learning (RL). It learns action detection by training an agent that iteratively picking an observation location and deciding whether to emit or refine a candidate action after observation. In this work, an end-to-end Transformer-based detector significantly different from [23] is proposed. While [23] is restricted to a manner of one-by-one prediction due to the recurrent nature of RNN, our method can decode all action instances in parallel. In addition, our method is fully differentiable, whereas the RL-based method is not.

Transformer. Transformers [18] have achieved great success in natural language processing. The core of Transformer is the self-attention mechanism that aggregates non-local information through an input-dependant weighted sum of features at all locations. Compared with convolutions, self-attention can aggregate global context at once, instead of stacking multiple layers. Recently, many works have revealed the great potential of Transformers in video understanding tasks. For example, VideoBert [17] and Act-Bert [31] utilize Transformers to learn an joint representation for video and text. Zhou *et al.* [30] capture the temporal dependency with Transformer for video captioning. Girdhar [7] apply Transformer to model the relationship between spatial proposals for spatio-temporal action detection. In this paper, Transformer is used to capture temporal context information for temporal action detection. Specifically, We employ attention layers to model the relationship between video snippets, the relationship between snippets and actions, and the relationship between actions. Different from many previous works, we introduce a temporal deformable attention layer that adaptively attends to a few key snippets instead of all snippets. Therefore, context information with-

out excessive computation cost.

3. TadTR

TadTR is constructed on video features encoded with a pre-trained video classification network (e.g. I3D [4]). Fig. 3 shows the overall architecture of TadTR. TadTR takes the video features and the temporal position encoding as input and outputs a set of action predictions. It consists of a Transformer encoder to model the interactions between frames, a Transformer decoder to predict action segments, and a segment rescoring module to estimate the localization quality. A segment matching module is used for ground truth assignments during training.

3.1. Architecture

Transformer Encoder. Let $X_V \in \mathbb{R}^{T \times C_V}$ denotes the video feature sequence, where T and C_V are the length and dimension, respectively. A 1D convolutional layer with kernel size 1 is applied to reduce its dimension to C . The Transformer encoder models the relation between different temporal locations and outputs a feature sequence $X_E \in \mathbb{R}^{T \times C}$ enhanced with temporal context. As depicted in Fig. 3, it consists of L_E Transformer encoder layers of the homogeneous architecture, where the key component is the attention layer.

The primitive dense attention layer in [18] attends to all locations in an input feature sequence, suffering from high computation cost and slow convergence. To mitigate these issues, we employ a temporal deformable attention (TDA) layer that only attends to a small set of temporal locations around a reference location in the feature sequence. Given an input feature sequence $X \in \mathbb{R}^{T \times C}$, let $p_q \in [0, 1]$, $z_q \in \mathbb{R}^C$ and $X(p_q) \in \mathbb{R}^C$ denote the coordinate of the reference point, the query feature at p_q and the input feature at p_q respectively. The TDA feature $TDA(z_q, X)$ is formulated by

$$\sum_{m=1}^M \mathbf{W}_m^O \left[\sum_{k=1}^K A_{mqk} \mathbf{W}_m^V X(p_q + \Delta p_{mqk}) \right], \quad (1)$$

where M is the number of attention heads, K is the number of attended points. $A_{mqk} \in [0, 1]$ is the normalized attention weight, $\mathbf{W}_m^O \in \mathbb{R}^{C \times (C/M)}$ and $\mathbf{W}_m^V \in \mathbb{R}^{(C/M) \times C}$ are learnable weights. $\Delta p_{mqk} \in [0, 1]$ is the sampling offset. Note that $p_q + \Delta p_{mqk}$ is fractional, so linear interpolation is used. \mathbf{W}_m^V maps the interpolated features to key features. Following [32], the attention weight A_{mqk} and the sampling offset Δp_{mqk} are mapped from the query feature z_q by linear projection. The output of the TDA layer has the same length as the input. When computing a location in the output, the input feature in the location acts as the query feature and the reference point is the location itself.

Besides the video features, a temporal position embedding $X_P \in \mathbb{R}^{T \times C}$ is also passed onto the encoder since

the Transformer is insensitive to the ordering of temporal locations. In this paper, we use the sinusoidal position embedding:

$$X_P(t, i) = \begin{cases} \sin \frac{t}{10000^{i/C}} & i \text{ is even} \\ \cos \frac{t}{10000^{(i-1)/C}} & i \text{ is odd} \end{cases}. \quad (2)$$

The positional encoding is added to the input of each attention layer.

Transformer Decoder. The decoder takes as inputs the encoder features X_E and N_q learnable action queries $Q = \{q_i\}_{i=1}^{N_q}$ and transforms these queries to N_q action predictions $\hat{Y} = \{\hat{y}_i\}$. As illustrated in Fig. 3, the decoder consists of L_D sequential decoder layers. In each decoder layer, self-attention and temporal deformable attention are both used. The self-attention layer models the relation between action queries and updates their features. To make an action prediction, each query needs to extract relevant context information from the video. To do that, we pass both the encoder features X_E and the query feature to the TDA layer. TDA has the same formulation as Equation 1. The key features are from X_E . Differently, the query feature is not from the video but automatically learned and the coordinate of the reference point is predicted from the query feature by non-linear projection. The reference point can be seen as the initial estimation of the center of the corresponding action segment. Based on the output of each decoder layer, we apply two multi-layer perceptrons (MLPs) to predict the classification probabilities \hat{p}_i and the temporal locations \hat{s}_i of the associated detection \hat{y}_i for each query q_i . The ground truth assignment is determined by the sequence matching module described in Sec. 3.2.

Segment Rescoring. One challenge of temporal action detection is the extreme scale (duration) variation of action instances, ranging from a few seconds to several minutes. Although the attention mechanism can dynamically attend features in different ranges, it cannot perfectly align the receptive field with the span of target actions. As a result, the confidence scores of the detections may be unreliable. An example is shown in Fig. 4.

To mitigate this issue, the segment rescoring module extracts features aligned with the span and predicts a new confidence score upon them. Given the encoder feature sequence X_E and a predicted segment \hat{s}_i by the decoder, we first apply temporal RoIAlign [8] upon X_E to obtain the aligned features $X_{s_i} \in \mathbb{R}^{\tau \times C}$ within the interval defined by s_i from X_E . Here, τ is the number of bins for RoIAlign. Then, an MLP is used to predict the target confidence score \hat{g}_i , supervised by the maximum IoU g_i (intersection over union) between s_i and all ground truth action instances.

Note that the number of detections produced by our method is small (no greater than 30). Therefore, segment

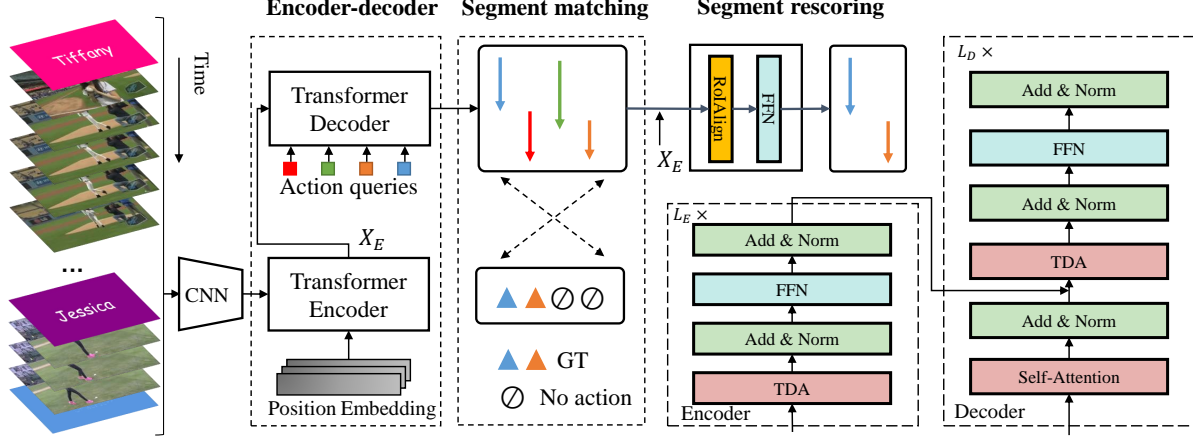


Figure 3. The architecture of TadTR. It takes the video features extracted with a CNN and position embedding as inputs and decodes a set of action predictions in parallel via a Transformer. The segment matching module supervises the predictions during training. The segment rescoring module estimates the IoU with its best-matched ground truth of a prediction for reranking and filtering. FFN is short for feed-forward network, which is a fully connected layer with activation.



Figure 4. The Transformer may produce detections with unreliable confidence scores. Here, a prediction with lower overlap with the curling action has a higher score than a more accurate prediction (0.50 vs. 0.39).

rescoring will not introduce much time cost, which is validated in the experiments.

Segment Refinement. Transformer is able to capture context information. However, the predicted action boundaries might be unsatisfactory for lack of locality. Therefore, we introduce a refinement mechanism to improve the localization performance. Based on the action segment $\hat{s}_i^{(l)} = (\hat{t}_i^{(l)}, \hat{d}_i^{(l)})$ predicted by the l -th ($1 \leq l \leq L_D - 1$) decoder layer, the $(l + 1)$ -th decoder layer refine its locations to make a new segment $\hat{s}_i^{(l+1)} = (\hat{t}_i^{(l+1)}, \hat{d}_i^{(l+1)})$:

$$\hat{t}_i^{(l+1)} = \sigma(\Delta t_i^{(l+1)} + \sigma^{-1}(\hat{t}_i^{(l)})) \quad (3)$$

$$\hat{d}_i^{(l+1)} = \sigma(\Delta d_i^{(l+1)} + \sigma^{-1}(\hat{d}_i^{(l)})), \quad (4)$$

where $\hat{t}_i^{(l)}$ and $\hat{d}_i^{(l)}$ are the coordinate of the center and the length of $\hat{s}_i^{(l)}$, respectively. $\Delta t_i^{(l+1)}$ and $\Delta d_i^{(l+1)}$ are the predicted offsets. $\sigma(\cdot)$ and $\sigma^{-1}(\cdot)$ are the sigmoid and the inverse sigmoid function, respectively.

For convenience, we denote TadTR without segment rescoring and interactive segment refinement as *TadTR-base*.

3.2. Training and Inference

Segment Matching. The segment matching module determines the targets assigned to each detection during training. Inspired by DETR [3] in object detection, we frame it as a set-to-set bipartite matching problem and solve it with the Hungarian algorithm.

Let $Y = \{y_j\}_{j=1}^{N_q}$ be a set of ground truth actions padded with \emptyset (no action) and π be the permutation that assigns y_j to $\hat{y}_{\sigma(y_j)}$. Bipartite matching aims to find a permutation that minimizes the overall matching cost:

$$\hat{\pi} = \arg \min \sum_{j=1}^{N_q} \mathcal{C}(y_j, \hat{y}_{\pi(j)}). \quad (5)$$

The matching cost considers the classification probabilities and the distance between ground truth and predicated segments. Specifically, $\mathcal{C}(y_j, \hat{y}_{\pi(j)})$ is defined as

$$-\mathbb{1}_{c_j \neq \emptyset}[(\hat{p}_{\pi(j)}(c_j) + \mathcal{L}_{seg}(s_j, \hat{s}_{\pi(j)})), \quad (6)$$

where c_j and s_j are the class label and the temporal locations of y_j . $\mathcal{L}_{seg}(s_j, \hat{s}_{\pi(j)})$ is the distance between the predicted location and the ground truth location, defined as

$$\lambda_{iou} \mathcal{L}_{iou}(s_j, \hat{s}_{\pi(j)}) + \lambda_{coord} \mathcal{L}_{L1}(s_j, \hat{s}_{\pi(j)}) \quad (7)$$

where \mathcal{L}_{L1} is the L_1 distance and \mathcal{L}_{iou} is the IoU loss. λ_{iou} and λ_{coord} are hyper-parameters.

Through the set-based segment matching, each ground truth will be assigned to only one prediction, thus avoiding duplicate predictions. This brings two merits. First, TadTR does not rely on the non-differentiable non-maximal suppression (NMS) for post-processing and enjoys end-to-end training. Second, we can make sparse predictions with limited queries (e.g. 10) instead of dense predictions in many

previous works (*e.g.* tens of thousands for BMN [10] and G-TAD [21]), which saves the computation cost.

Loss Functions. Once the ground truth assignment determined, we optimize the network by minimizing the following multi-part loss functions:

$$\mathcal{L} = \sum_{j=1}^{N_q} [-\log \hat{p}_{\hat{\pi}(j)}(c_j) + \mathbb{1}_{c_j \neq \emptyset} \mathcal{L}_{seg}(s_j, \hat{s}_{\hat{\pi}(j)}) + \lambda_{rescore} \mathcal{L}_{L1}(\hat{g}_{\hat{\pi}(j)}, g_{\hat{\pi}(j)})], \quad (8)$$

where the first two items optimize the detections from the decoder and the last optimizes the outputs of segment rescoring. $\hat{\pi}$ is the solution of equation (5). $\lambda_{rescore}$ is a hyper-parameter.

Inference. During inference, we ignore the action predictions from all but the last decoder layer. The production of the confidence score predicted by the rescoring module and the classification probabilities predicted by the decoder is used for detection ranking.

4. Experiments

4.1. Experimental Setup

Datasets and Evaluation Metrics. We conduct experiments on THUMOS14 [9], ActivityNet-1.3 [2] and HACS Segments [26]. THUMOS14 is built on videos from 20 sports action classes. It contains 200 and 213 untrimmed videos for training and testing. There are 3007 and 3358 action instances on the two sets. ActivityNet-1.3 and HACS Segments share the same 200 classes of daily activities. Both datasets are split into three sets: training, validation, and testing. The numbers of videos in these sets are 10024, 4926, and 5044 respectively on ActivityNet-1.3, and 37613, 5981, and 5987 on HACS Segments. On both datasets, the annotations on the testing set are reserved by the organizers. Therefore, we evaluate the validation set.

Following conventions, the mean average precision (mAP) is used for performance evaluation. On THUMOS14, the IoU thresholds for computing mAPs are [0.3 : 0.7 : 0.1], and the mAP at the threshold 0.5 is the primary metric. On the other two datasets, we report mAPs at the thresholds {0.5, 0.75, 0.95} and the average mAP at the thresholds [0.5 : 0.95 : 0.05].

Video Feature Extraction. For experiments on HACS Segments, we directly use the official I3D features¹, which are extracted with I3D trained on Kinetics at 2FPS. On the other datasets, we use the commonly used features in previous works. On THUMOS14, the two-stream I3D [4] networks pre-trained on Kinetics [4] are taken as the video encoder, and the features are extracted every 8 frames. On

¹http://hacs.csail.mit.edu/hacs_segments_features.zip

ActivityNet-1.3, we use the two-stream TSN [19] features extracted at 5FPS. Following previous works [10, 21], we resize the video features to a fixed length of 100 via interpolation on ActivityNet-1.3 and HACS Segments.

Implementation Details. The number of queries is set to 30, 10, and 30 on THUMOS14, ActivityNet-1.3, and HACS Segments respectively, according to the statistics on each dataset’s training set. L_E and L_D are set to 2 and 4, respectively. The loss weights λ_{iou} , λ_{coord} and $\lambda_{rescore}$ are set to 2, 5 and 5 respectively. We use deformable attention [32] as the self-attention module instead of scaled dot-product attention, as the former shows faster convergence. TadTR is trained using AdamW [14] optimizer. The initial learning rate is 2×10^{-4} and scaled by a factor of 0.1 after training for a certain number of epochs. We train the models for 60, 15 and 30 epochs and decrease the learning rate after 50, 12, and 25 epochs on THUMOS14, ActivityNet-1.3, and HACS Segments respectively. The batch size is set to 16. For run time measurement, we run methods on the full testing set on THUMOS14 with batch size set to 1 on a workstation with a single Tesla P100 GPU card, and Intel(R) Xeon(R) CPU E5-2682 v4 @ 2.50GHz. The feature extraction time is not included. Note that the inference time is related to the length of a video. The average length of videos on THUMOS14 is 217 seconds.

4.2. Main Results

THUMOS14. Tab. 1 demonstrates the temporal action detection performance and run time comparison on the testing set of THUMOS14. We measure the run time of methods with publicly available implementations on the same hardware (a single P100 GPU). We observe that (1) Compared with previous methods, TadTR achieves the best performance in terms of mAP at IoU=0.5 and average mAP. (2) Compared with recent methods with close performance, such as A2Net [22] and MR [27], TadTR runs much faster. Specifically, TadTR is $4.2 \times$ faster than the second-best method MR [27]. This indicates TadTR is more efficient. (3) When combined with a post-processing method P-GCN, TadTR achieves an mAP of 52.8% at IoU=0.5. In comparison, BSN and G-TAD achieve inferior performance when combined with P-GCN. The above results indicate that TadTR is both accurate and efficient. We also note that many other methods are composed of multiple networks for different functions, while TadTR is able to perform action detection with only a single unified network.

HACS Segments. This is a recently introduced dataset, therefore the results of many previous methods on this dataset are not available. We report the performance of SSN [28] and G-TAD [21]. The results of SSN are from [26]. The results of G-TAD are obtained with our im-

Method	Single-network	E2E	0.3	0.4	0.5	0.6	0.7	Avg.	Run Time (ms)
Yeung <i>et al.</i> [23]	✓	✓	36.0	26.4	17.1	-	-	-	195
Yuan <i>et al.</i> [24]	-	-	36.5	27.8	17.8	-	-	-	-
SSAD [11]	✓	-	43.0	35.0	24.6	-	-	-	-
R-C3D [20]	✓	-	44.8	35.6	28.9	-	-	-	-
SSN [29]	-	-	51.9	41.0	29.8	-	-	-	-
TAL-Net [5]	✓	-	53.2	48.5	42.8	33.8	20.8	39.8	-
BSN [12]	-	-	53.5	45.0	36.9	28.4	20.0	36.8	2065
MGG [13]	-	-	53.9	46.8	37.4	29.5	21.3	37.8	-
BMN [10]	-	-	56.0	47.4	38.8	29.7	20.5	38.5	483
G-TAD [21]	-	-	54.5	47.6	40.2	30.8	23.4	39.3	4440
BC-GNN [1]	-	-	57.1	49.1	40.4	31.2	23.1	40.2	-
MR [27]	-	-	53.9	50.7	45.4	38.0	28.5	43.3	644
A2Net [22]	✓	-	58.6	54.1	45.5	32.5	17.2	41.6	1554
TadTR (Ours)	✓	✓	59.6	55.0	46.6	35.7	24.3	44.3	155
BSN+P-GCN [25]	-	-	63.6	57.8	49.1	-	-	-	7143
G-TAD+P-GCN [20]	-	-	66.4	60.4	51.6	37.6	22.9	47.8	-
TadTR+P-GCN (Ours)	-	-	66.3	60.7	52.8	40.3	25.5	49.1	7728

Table 1. Comparison with state-of-the-art methods on THUMOS14. Run time is the average inference time per video. For proposal generation methods (BSN, MGG, BMN, G-TAD, MR, BC-GNN), the run time of the proposal classification stage is not counted. E2E is short for end-to-end.

plementation based on its official code² using I3D features. Our method achieves an average mAP of 29.51%, which clearly outperforms SSN (+10.54% mAP) and G-TAD (+2.03% mAP). The results again illustrate the superiority of TadTR.

ActivityNet-1.3. In Tab. 3, we compare temporal action detection performance of different methods on the validation set of ActivityNet-1.3. Some methods, such as G-TAD, only implements action proposal generation and can not produce action detections without external action classifiers. We divide the methods into two groups according to whether external action classifiers are used. Being simple and end-to-end trainable, TadTR achieves an average mAP of 27.16%, which is stronger than more complicated methods such as TAL-Net [5] and P-GCN [25].

To enhance the detection performance, we also try combining TadTR with an ensemble of action classifiers trained by [29] following previous works [22, 21]. To be concrete, we pass the detections by TadTR to the classifiers and fuse the classification scores of TadTR and the classifiers by multiplication. When fused with [28], TadTR enjoys a significant performance boost to an average mAP of 31.32%. The results are better than recent methods such as MR [27] and A2Net [22] that are also combined with [29]. Our results are inferior to that of G-TAD. We conjecture that there are two possible reasons. First, Transformer requires a large number of samples to train. An insufficient number of samples per class (77, compared with 150 on THUMOS14 and 529 on HACS Segments) restricts the performance of

TadTR. Second, the context information on ActivityNet-1.3 is limited due to the small number of action instances per video. On average, the ActivityNet training set has only 1.5 instances per video. By contrast, the training sets of THUMOS14 and HACS Segments have 15.4 and 2.8 instances per video, respectively.

4.3. Analysis

The importance of context information. The key of Transformer is the self-attention mechanism that incorporates the context in a video sequence. In TadTR, we leverage two kinds of context, snippet-level context from all snippets and instance-level context from all action queries, which are captured by Transformer encoder and the self-attention layer in Transformer decoder respectively. By removing Transformer encoder, we get a variant “TadTR w/o encoder”. By removing the self-attention layer in the decoder, we get a variant “TadTR w/o instance-level context”. We report the performance of the two variants in Tab. 2. It is observed that removing the encoder leads to a significant performance drop of 3.93% in terms of average mAP. It indicates that the Transformer encoder is crucial for our model, as the decoder requires long-range and adaptive context to reason the relations between the actions and the video. Removing instance-level context, the average mAP drops by 1.88%. We conclude that the context information from other action instances is also helpful for action detection.

Transformer encoder v.s. CNN encoder. We try replacing the Transformer encoder with a 1D CNN encoder, which

²<https://github.com/frostinassiky/gtad/tree/hacs>

Method	0.5	0.75	0.95	Avg.
SSN [29]	28.82	18.80	5.32	18.97
G-TAD [21]	41.08	27.59	8.34	27.48
<i>Ours</i>				
TadTR	45.03	30.86	11.01	30.87
TadTR w/o encoder	39.65	26.99	9.08	26.94
TadTR w/o instance-level context	43.11	29.97	10.43	29.70
TadTR with a 1D CNN encoder	40.96	28.00	9.73	27.95
TadTR w/o segment rescoring	42.10	28.44	10.23	28.51
TadTR w/o segment refinement	39.89	28.03	9.54	27.65

Table 2. Comparison of different methods and different variants of TadTR on the validation set of HACS Segments.

Method	Single-network	E2E	0.5	0.75	0.95	Avg.
CDC [15]	-	-	43.83	25.88	0.21	22.77
R-C3D [20]	✓	-	26.8	-	-	-
SSN [28]	-	-	39.12	23.48	5.49	23.98
TAL-Net [5]	✓	-	38.23	18.30	1.30	20.22
P-GCN [25]	-	-	42.90	28.14	2.47	26.99
TadTR (Ours)	✓	✓	41.53	27.40	5.75	27.16
<i>Combined with external action classifiers</i>						
P-GCN [25]	-	-	48.26	33.16	3.27	31.11
MR [27]	-	-	43.47	33.91	9.21	30.12
A2Net [22]	-	-	43.55	28.69	3.70	27.75
G-TAD [21]	-	-	50.36	34.60	9.02	34.09
TadTR (Ours)	-	-	47.57	31.65	7.98	31.32

Table 3. Comparison of different methods on ActivityNet-1.3. Methods in the second group are combined with an ensemble of action classifiers [29].

is common for temporal modeling in previous TAD methods. The 1D CNN encoder is composed of two 1D convolutional layers with 256 filters of kernel size 9 and ReLU activation. This variant is denoted as “TadTR with a 1D CNN encoder”. As can be observed in Tab. 2, the performance of this variant is worse than TadTR (-2.92% average mAP). We also explore deeper CNNs and larger convolution kernels, but no improvement is observed. The results show that 1D CNN is inferior to Transformer encoder. The reason might be that the fixed receptive field of convolution prevents adaptive context extraction.

Effects of segment rescoring and segment refinement. We study the effects of iterative segment refinement and segment rescoring by removing them from TadTR individually, resulting in 2 different model variants. Their results on HACS Segments is presented in Tab. 2. Comparing TadTR w/o segment rescoring and TadTR, we observe that segment rescoring leads to improvements of all metrics. Specifically, the improvements are 2.93%, 2.42%, 0.78%, and 2.36% in terms of mAP at IoU 0.5, 0.75, 0.95 and the average mAP. Several qualitative examples are presented in Fig. 5 to show how segment rescoring helps. It is able to produce more reliable confidence scores for the action predictions

by Transformer, owing to explicit feature alignment. Comparing TadTR w/o segment refinement and TadTR, we find this component helpful for improving the localization accuracy. It improves the mAP at the strict threshold of 0.95 by a large margin of 2.47%. The mAPs at other thresholds are also consistently improved.

Besides the detection performance, another important aspect is the time cost of the detector. For easier comparison, we use the same protocol used in Fig. 1 and Tab. 1 for run time measurement. The average time cost per video is 130 ms for TadTR-base. Adding the rescoring module will increase the average time cost to 141 ms, i.e. an increase of 8.5%. With segment refinement enabled, the full model average time cost becomes 155 ms, which is still very efficient compared with state-of-the-art methods.

The meaning of action queries. Fig. 6 illustrates the distribution of locations and scales (lengths) of output actions associated with each action query. We observe that each query produces action predictions in certain locations and scales. Different locations and scales are covered by a small number of queries. It means that the detector learns the distribution of actions in the training dataset. This is more flexible and efficient than the handcrafted anchor design in previous

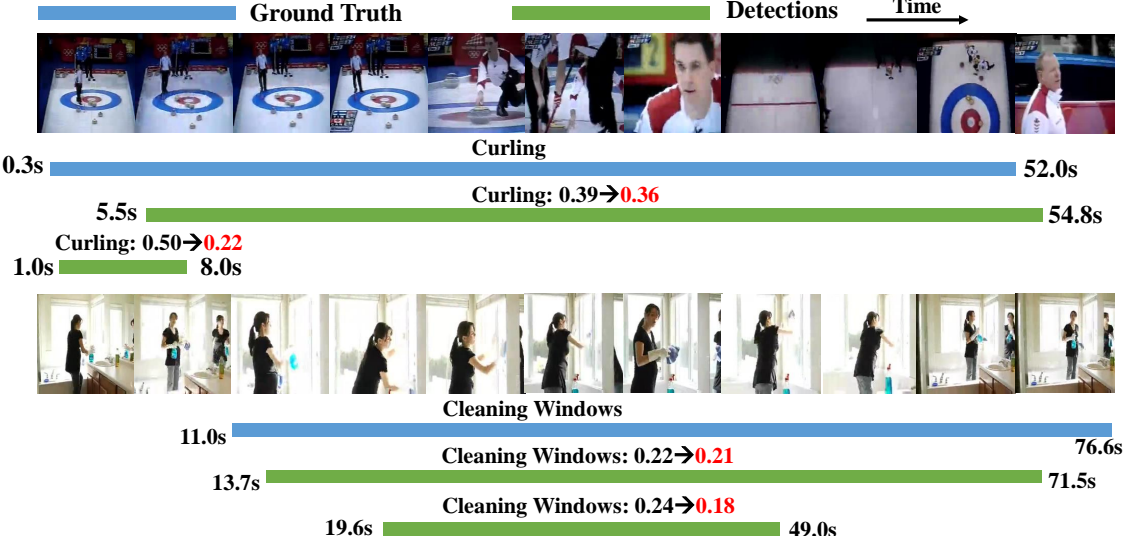


Figure 5. Segment rescore improves the ranking of detections. In each of the above cases, the more accurate obtains a lower score than the less accurate one before rescore. With the new scores (red color) applied, the ranking order turns satisfactory.

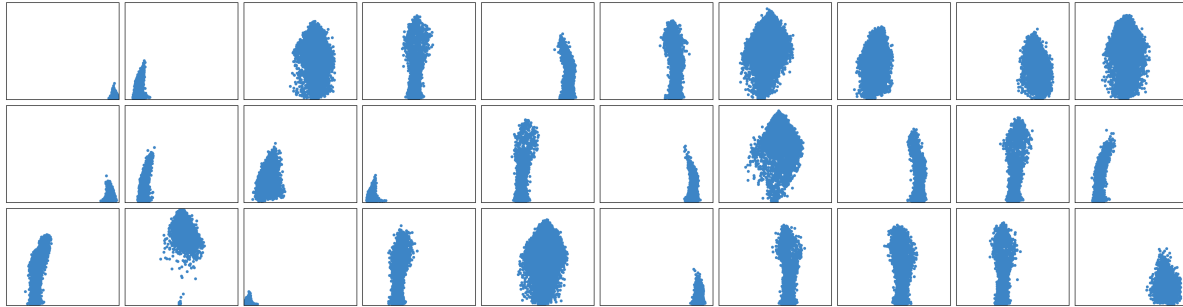


Figure 6. Distribution of all output actions on all videos from HACS Segments validation set for 30 query slots with action queries. In each 1-by-1 square, an action prediction is represented as a point, and the horizontal and vertical coordinates are the coordinate of the center and the length normalized by the video length.

L_E	L_D	0.5	0.75	0.95	Avg.
2	4	45.03	30.86	11.01	30.87
4	4	44.63	30.39	10.76	30.39
6	4	40.55	27.55	9.88	27.63
2	2	42.10	29.05	9.57	28.84
2	4	45.03	30.86	11.01	30.87
2	6	45.20	30.82	10.67	30.74

Table 4. Effect of numbers of encoder layers and decoder layers. The detection performance is evaluated on HACS Segments.

methods.

Effects of numbers of encoder layers and decoder layers. We evaluate TadTR with different numbers of encoder layers (L_E) and decoder layers (L_D) and report results in Tab. 4. With L_D fixed, the best performance is achieved when L_E is 2. Larger L_E gives inferior results probably due to the difficulty of training. Therefore, we set L_E to 2. With L_E fixed, the average mAP increases by 2.03% when

L_D increases from 2 to 4. Larger L_D gives a slightly lower performance. Therefore we suggest setting L_D to 4.

5. Conclusion

We propose TadTR, a new end-to-end framework for temporal action detection based on Transformer. It views the TAD task as a direct set-prediction problem and decodes all action instances in parallel, significantly different from previous works. It simplifies the pipeline of TAD and removes hand-crafted designs such as anchor setting and post-processing. Extensive experiments are conducted to validate the performance and efficiency of TadTR and the effectiveness of different components. TadTR achieves state-of-the-art or competitive performance on HACS Segments, THUMOS14 and ActivityNet-1.3 while running significantly faster. We hope that our work could trigger the development of simple and efficient models for temporal action detection.

References

- [1] Yueran Bai, Yingying Wang, Yunhai Tong, Yang Yang, Qiyue Liu, and Junhui Liu. Boundary content graph neural network for temporal action proposal generation. In *ECCV*, pages 121–137, 2020.
- [2] Fabian Caba Heilbron, Victor Escorcia, Bernard Ghanem, and Juan Carlos Niebles. Activitynet: A large-scale video benchmark for human activity understanding. In *CVPR*, pages 961–970, 2015.
- [3] Nicolas Carion, Francisco Massa, Gabriel Synnaeve, Nicolas Usunier, Alexander Kirillov, and Sergey Zagoruyko. End-to-end object detection with transformers. In *ECCV*, pages 213–229, 2020.
- [4] Joao Carreira and Andrew Zisserman. Quo vadis, action recognition? a new model and the kinetics dataset. In *CVPR*, pages 4724–4733, 2017.
- [5] Yu-Wei Chao, Sudheendra Vijayanarasimhan, Bryan Seybold, David A Ross, Jia Deng, and Rahul Sukthankar. Rethinking the faster r-cnn architecture for temporal action localization. In *CVPR*, pages 1130–1139, 2018.
- [6] Xiyang Dai, Bharat Singh, Guyue Zhang, Larry S Davis, and Yan Qiu Chen. Temporal context network for activity localization in videos. In *ICCV*, pages 5727–5736, 2017.
- [7] Rohit Girdhar, Joao Carreira, Carl Doersch, and Andrew Zisserman. Video action transformer network. In *Proceedings of the IEEE/CVF Conference on Computer Vision and Pattern Recognition*, pages 244–253, 2019.
- [8] Kaiming He, Georgia Gkioxari, Piotr Dollár, and Ross Girshick. Mask r-cnn. In *ICCV*, pages 2961–2969, 2017.
- [9] YG Jiang, Jingen Liu, A Roshan Zamir, G Toderici, I Laptev, Mubarak Shah, and Rahul Sukthankar. Thumos challenge: Action recognition with a large number of classes, 2014.
- [10] Tianwei Lin, Xiao Liu, Xin Li, Errui Ding, and Shilei Wen. Bmn: Boundary-matching network for temporal action proposal generation. In *ICCV*, pages 3889–3898, 2019.
- [11] Tianwei Lin, Xu Zhao, and Zheng Shou. Single shot temporal action detection. In *ACM MM*, pages 988–996, 2017.
- [12] Tianwei Lin, Xu Zhao, Haisheng Su, Chongjing Wang, and Ming Yang. Bsn: Boundary sensitive network for temporal action proposal generation. In *ECCV*, September 2018.
- [13] Yuan Liu, Lin Ma, Yifeng Zhang, Wei Liu, and Shih-Fu Chang. Multi-granularity generator for temporal action proposal. In *CVPR*, pages 3604–3613, 2019.
- [14] Ilya Loshchilov and Frank Hutter. Decoupled weight decay regularization. In *ICLR*, 2017.
- [15] Zheng Shou, Jonathan Chan, Alireza Zareian, Kazuyuki Miyazawa, and Shih-Fu Chang. Cdc: Convolutional-deconvolutional networks for precise temporal action localization in untrimmed videos. In *ICCV*, pages 1417–1426, 2017.
- [16] Zheng Shou, Dongang Wang, and Shih-Fu Chang. Temporal action localization in untrimmed videos via multi-stage cnns. In *CVPR*, pages 1049–1058, 2016.
- [17] Chen Sun, Austin Myers, Carl Vondrick, Kevin Murphy, and Cordelia Schmid. Videobert: A joint model for video and language representation learning. In *Proceedings of the IEEE/CVF International Conference on Computer Vision*, pages 7464–7473, 2019.
- [18] Ashish Vaswani, Noam Shazeer, Niki Parmar, Jakob Uszkoreit, Llion Jones, Aidan N. Gomez, Łukasz Kaiser, and Illia Polosukhin. Attention is all you need. In *NIPS*, pages 5998–6008, 2017.
- [19] Limin Wang, Yuanjun Xiong, Zhe Wang, Yu Qiao, Dahua Lin, Xiaoou Tang, and Luc Van Gool. Temporal segment networks: Towards good practices for deep action recognition. In *ECCV*, pages 20–36, 2016.
- [20] Huijuan Xu, Abir Das, and Kate Saenko. R-c3d: region convolutional 3d network for temporal activity detection. In *ICCV*, pages 5794–5803, 2017.
- [21] Mengmeng Xu, Chen Zhao, David S Rojas, Ali Thabet, and Bernard Ghanem. G-TAD: Sub-graph localization for temporal action detection. In *CVPR*, pages 10156–10165, 2020.
- [22] Le Yang, Houwen Peng, Dingwen Zhang, Jianlong Fu, and Junwei Han. Revisiting anchor mechanisms for temporal action localization. *IEEE Transactions on Image Processing*, 29:8535–8548, 2020.
- [23] Serena Yeung, Olga Russakovsky, Greg Mori, and Li Fei-Fei. End-to-end learning of action detection from frame glimpses in videos. In *CVPR*, pages 2678–2687, 2016.
- [24] Ze-Huan Yuan, Jonathan C Stroud, Tong Lu, and Jia Deng. Temporal action localization by structured maximal sums. In *CVPR*, volume 2, page 7, 2017.
- [25] Runhao Zeng, Wenbing Huang, Mingkui Tan, Yu Rong, Peilin Zhao, Junzhou Huang, and Chuang Gan. Graph convolutional networks for temporal action localization. In *ICCV*, pages 7094–7103, 2019.
- [26] Hang Zhao, Antonio Torralba, Lorenzo Torresani, and Zhicheng Yan. HACS: human action clips and segments dataset for recognition and temporal localization. In *ICCV*, pages 8667–8677, 2019.
- [27] Peisen Zhao, Lingxi Xie, Chen Ju, Ya Zhang, Yanfeng Wang, and Qi Tian. Bottom-up temporal action localization with mutual regularization. In *ECCV*, 2020.
- [28] Yue Zhao, Yuanjun Xiong, Limin Wang, Zhirong Wu, Xiaoou Tang, and Dahua Lin. Temporal action detection with structured segment networks. *ICCV*, pages 2914–2923, 2017.
- [29] Yue Zhao, Bowen Zhang, Zhirong Wu, Shuo Yang, Lei Zhou, Sijie Yan, Limin Wang, Yuanjun Xiong, Wang Yali, Dahua Lin, Yu Qiao, and Xiaoou Tang. CUHK & ETHZ & SIAT submission to ActivityNet challenge 2017. *arXiv preprint arXiv:1710.08011*, pages 20–24, 2017.
- [30] Luwei Zhou, Yingbo Zhou, Jason J Corso, Richard Socher, and Caiming Xiong. End-to-end dense video captioning with masked transformer. In *CVPR*, pages 8739–8748, 2018.
- [31] Linchao Zhu and Yi Yang. Actbert: Learning global-local video-text representations. In *Proceedings of the IEEE/CVF Conference on Computer Vision and Pattern Recognition*, pages 8746–8755, 2020.
- [32] Xizhou Zhu, Weijie Su, Lewei Lu, Bin Li, Xiaogang Wang, and Jifeng Dai. Deformable detr: Deformable transformers for end-to-end object detection. In *ICLR*, 2021.